

Search for the Higgs boson in the VH(bb) channel using the ATLAS detector

David López Mateos* on behalf of the ATLAS Collaboration

Harvard University

E-mail: dlopez@physics.harvard.edu

A search for the $b\bar{b}$ decay of the Standard Model Higgs boson is performed with the ATLAS experiment using the full dataset recorded at the LHC in Run 1. The integrated luminosities used from pp collisions at $\sqrt{s} = 7$ and 8 TeV are 4.7 and 20.3 fb^{-1} , respectively. The processes considered are associated $(W/Z)H$ production, with $W \rightarrow \ell\nu$, $Z \rightarrow \ell\ell$ ($\ell = e, \mu$), and $Z \rightarrow \nu\nu$. No significant excess is observed on top of the Standard Model (SM) backgrounds. For $m_H = 125 \text{ GeV}$, a 95% CL upper limit of 1.4 times the SM expectation is set on the cross section times branching ratio for $pp \rightarrow (W/Z)(H \rightarrow b\bar{b})$. The corresponding limit expected in the absence of signal is 1.3. The ratio of the measured signal strength to the SM expectation is found to be $\mu = 0.2 \pm 0.5(\text{stat.}) \pm 0.4(\text{syst.})$. The analysis procedure is validated by a measurement of the yield of $(W/Z)Z$ production, with $Z \rightarrow b\bar{b}$, from which the ratio of the observed signal strength to the SM expectation is found to be $\mu^{VZ} = 0.9 \pm 0.2$.

*The European Physical Society Conference on High Energy Physics -EPS-HEP2013
18-24 July 2013
Stockholm, Sweden*

*Speaker.

1. Introduction

The discovery of a new particle with a mass of approximately 125 GeV at the ATLAS [1] and CMS [2] experiments at the LHC [3, 4] is a major milestone in our understanding of the Standard Model (SM). The properties of this particle are consistent with those of the SM Higgs boson after the analysis of the full Run 1 dataset [5, 6, 7]. The ATLAS measurements have been performed in the bosonic decay modes ($H \rightarrow \gamma\gamma$, $H \rightarrow ZZ$, and $H \rightarrow WW$). Despite the main production mechanism and the $\gamma\gamma$ decay providing indirect evidence of its coupling to fermions, it is essential to obtain direct evidence of these couplings as predicted by the SM.

The $H \rightarrow b\bar{b}$ decay mode is predicted in the SM to have a branching ratio of 58% for $m_H = 125$ GeV [8]. An inclusive search for this decay is not feasible at the LHC because of the overwhelming background from jet production. The associated production of a Higgs boson with a vector boson, W or Z (collectively referred to as V), offers an alternative because leptonic decays, $W \rightarrow \ell\nu$, $Z \rightarrow \ell\ell$ ($\ell = e, \mu$), and $Z \rightarrow \nu\nu$, can be used effectively for triggering and background reduction purposes.

This note presents results of a search using the full dataset recorded by ATLAS during Run 1 of the LHC. This dataset consists of 4.7 fb^{-1} collected at a center-of-mass energy $\sqrt{s} = 7$ TeV in 2011 and 20.3 fb^{-1} collected at $\sqrt{s} = 8$ TeV in 2012. To validate the analysis, a measurement of the cross section of VZ production is also performed in the same final states and with the same event selection, with $H \rightarrow b\bar{b}$ replaced by $Z \rightarrow b\bar{b}$.

2. Event Selection

The analysis is performed for events containing zero, one, or two charged leptons (electrons or muons), targeting the $Z \rightarrow \nu\nu$, $W \rightarrow \ell\nu$, and $Z \rightarrow \ell\ell$ decays. Events are selected using hardware and software-level trigger algorithms that use E_T^{miss} (0-lepton channel), single-lepton identification (1-lepton, 2-lepton channels) and di-lepton identification (2-lepton channel). A b -tagging algorithm [9] is used to identify the jets from the $H \rightarrow b\bar{b}$ decay. Selection criteria for each channel are summarized in Table 1 and detailed in Ref. [10]. To improve the sensitivity, the three channels are split according to the vector boson transverse momentum (p_T^V) and the number of jets. Additional p_T^V -dependent cuts on the ΔR between the two b -tagged jets are applied to reject background, exploiting the correlation between the momenta of the vector and Higgs bosons. Five p_T^V bins are used in the 1-lepton and 2-lepton channels in the following ranges: 0-90 GeV, 90-120 GeV, 120-160 GeV, 160-200 GeV, > 200 GeV. In the 0-lepton channel, only the three highest bins are used, guaranteeing that the E_T^{miss} trigger selection has high efficiency.

Search regions analogous to those above but with one identified b -jet (1-tag) are used to constrain V +charm (c) backgrounds. Regions with no identified b -jets (0-tag) are used to study the modeling of V +light-quark production. A region with the same 2-lepton selection but requiring different flavor leptons (an electron and a muon) and $m_{\ell\ell} > 40$ GeV is used as a pure control region to understand $t\bar{t}$ background.

A loose selection on $m_{\ell\ell}$ in the 0-tag and 1-tag regions is used to estimate multijet backgrounds in the 2-lepton channel. In the 1-lepton channel, fits to the $m_T^{\ell V}$ (electron channel) and E_T^{miss} (muon channel) distributions are used for that purpose. The templates used for the multijet

Table 1: Event selection for the three channels [10]. $p_T^{\text{jet}_i}$ refers to the p_T of the i^{th} leading jet in p_T , \vec{E}_T^{miss} stands for the reconstructed missing transverse energy vector and \vec{p}_T^{miss} stands for the missing transverse momentum vector that is reconstructed using only tracks. In the 1-lepton selection, $m_T^{\ell V} = \sqrt{E_T^{\text{miss}} E_T^{\ell} (1 - \cos \Delta\phi(\vec{E}_T^{\text{miss}}, \ell))}$, where E_T^{ℓ} refers to the transverse energy of the lepton. In the 2-lepton selection, $m_{\ell\ell}$ refers to the invariant mass of the two leptons.

Object	0-lepton	1-lepton	2-lepton
Leptons	0 loose	1 tight + 0 loose	1 medium + 1 loose
Jets	2 b -tags, $p_T^{\text{jet}_1} > 45$ GeV, $p_T^{\text{jet}_2} > 20$ GeV, ≤ 1 additional jets		
Missing E_T	$E_T^{\text{miss}} > 120$ GeV $p_T^{\text{miss}} > 30$ GeV $\Delta\phi(\vec{E}_T^{\text{miss}}, \vec{p}_T^{\text{miss}}) < \pi/2$ $\min[\Delta\phi(\vec{E}_T^{\text{miss}}, \text{jet})] > 1.5$ $\Delta\phi(\vec{E}_T^{\text{miss}}, b\bar{b}) > 2.8$	$E_T^{\text{miss}} > 25$ GeV	$E_T^{\text{miss}} < 60$ GeV
Vector Boson	-	$m_T^{\ell V} < 120$ GeV	$83 < m_{\ell\ell} < 99$ GeV

background in these fits are obtained inverting certain lepton isolation criteria [10]. In the 0-lepton channel, the multijet background is estimated using yields in the regions defined by inverting the $\min[\Delta\phi(\vec{E}_T^{\text{miss}}, \text{jet})]$ and the $\Delta\phi(\vec{E}_T^{\text{miss}}, \vec{p}_T^{\text{miss}})$ cuts.

3. Fit Model

A number of systematic uncertainties affect the different search regions. In order to account for all the correlations, the results are obtained through an extended maximum likelihood fit [11] for all the backgrounds and the signal in a subset of the regions defined above (see Table 2.) The fit

Table 2: Search regions used in the fit [10]. The fit uses the yield only for certain regions (N) while the shape of the m_{bb} distribution is used in other regions (S).

	2-jet, 1-tag	3-jet, 1-tag	2-jet, 2-tag	3-jet, 2-tag	top different flavor
0-lepton (3 p_T^V bins)	N	N	S	S	-
1-lepton (5 p_T^V bins)	N	N	S	S	-
2-lepton (5 p_T^V bins)	N	N	S	S	N

uses information about the shape of the invariant mass distribution of the two tagged jets to improve the signal discrimination in search regions in which the purity of the signal is highest.

The normalization of all significant backgrounds ($V + c/b$ and $t\bar{t}$) is allowed to vary without constraints in the fit. The V +light and multijet normalizations are allowed to vary within constraints obtained using results in the 0-tag region. The normalization of other backgrounds are allowed to vary within constraints obtained using theoretical calculations as described in the next section.

Systematic uncertainties accounting for detector effects are taken to be fully correlated when relevant. The fit is sensitive to correlations through migrations among the different regions (e.g. a lower lepton efficiency will increase the Z +jets yield in 0-lepton and 1-lepton bins and decrease

it in 2-lepton bins) or among bins in the m_{bb} distributions in the 2-tag regions. Differences in the yields between two search regions can be caused by detector effects or by limitations in the modeling of the background processes. The fit includes nuisance parameters that account for such limitations too as discussed in the next section.

4. Background Modeling and Systematic Uncertainties

High statistics are available to study some of the most relevant backgrounds. The 0-tag and 1-tag regions allow for a careful study of the V +light-quark and V +heavy flavor backgrounds, as the different flavor region allows for top. Both 0-tag and 1-tag regions indicate a significant mismodeling of the distribution of $\Delta\phi$ between the selected jets in the leading-order (LO) simulations used [10]. The mismodeling is of similar magnitude and shape as expected going from LO to next-to-LO calculations in V +heavy flavor. A correction is thus applied to correct for this effect. The correction improves the description of many other variables in the 0-tag and 1-tag bin. One of those variables is p_T^V , shown in Fig. 1 for the 1-lepton channel, before and after the correction. A similar

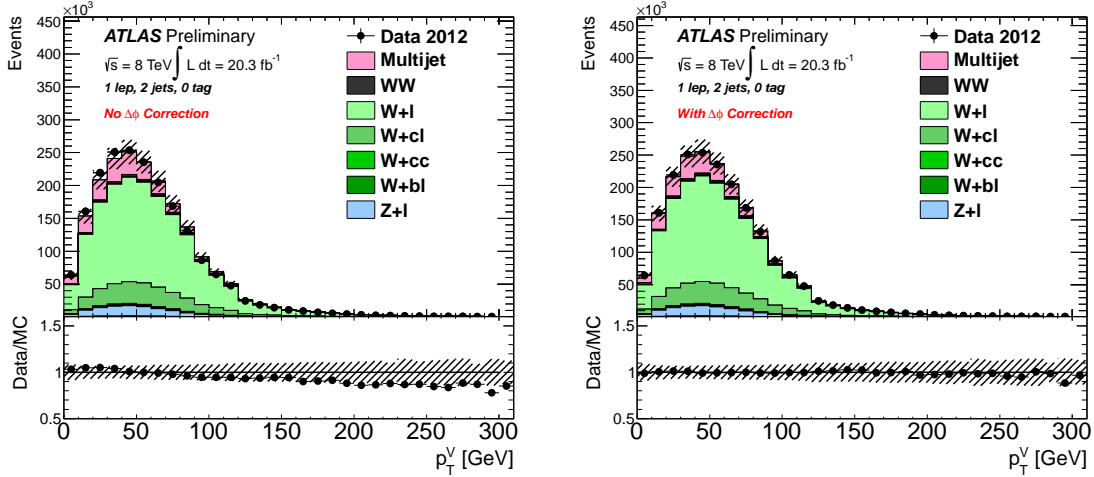


Figure 1: The p_T^V distribution in data and simulation for the 2-jet 0-tag control region of the 1-lepton channel, before (left) and after (right) reweighting the $\Delta\phi(\text{jet}_1, \text{jet}_2)$ distribution [10]. The background expectation is the prediction from the pre-fit simulation and the error bands represent systematic uncertainties in the simulation predictions prior to the fit.

study has been performed for $t\bar{t}$. Based on this study a correction to the top p_T is applied improving the agreement between data and simulation for kinematic variables in the $t\bar{t}$ control region [10].

Uncertainties in trigger and event selection, as well as lepton, jet and E_T^{miss} energy scale and resolution are accounted for using full kinematic correlations [10]. The uncertainty in the efficiency to identify a c -jet as a b -jet at high p_T dominates these uncertainties. However, the contribution of these detector uncertainties to the total systematic uncertainty is small compared to that of uncertainties in the modeling of backgrounds.

Modeling uncertainties are estimated on all distributions that enter the fit or the search region definition (p_T^V , 3-to-2-jet ratio, m_{bb}) and on the $\Delta\phi$ correction. Uncertainties are either based on

data/simulation comparisons (top p_T , p_T^V , $\Delta\phi$, m_{bb} for Z+jets, multijet), whenever pure samples are available in data, or on detailed simulation studies (e.g. 3-to-2-jet ratios.) simulation-based systematic uncertainties include variations in the underlying event and parton shower modeling, comparisons between the leading-order and next-to-leading order calculations, or between different generators. Details are available in Ref. [10].

5. Results

Fig. 2 shows the background-subtracted invariant mass distribution after all 2-tag regions and channels have been added (left) and when the addition is performed weighting by the expected S/B for an SM Higgs boson signal (right). The WZ and ZZ diboson background has not been subtracted.

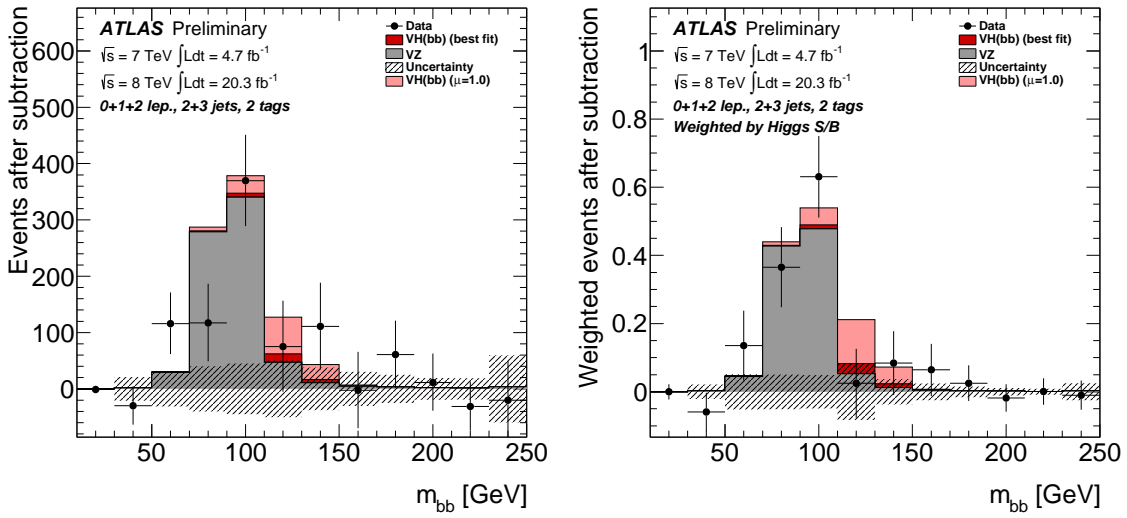


Figure 2: m_{bb} distribution after subtraction of all backgrounds except for the diboson processes (left). Also shown is the m_{bb} distribution where the contributions from each signal region are summed weighted by their respective values of Higgs-boson-signal over background ratio (right) [10]. Backgrounds are evaluated according to the results of the global Higgs-boson fit. The contribution from a hypothetical Higgs boson signal with $m_H = 125$ GeV is shown both with its fitted signal strength (“best fit”) and as expected for the SM cross section ($\mu = 1.0$). The hashed band represents the combined statistical and systematic uncertainty on the fitted background.

Fig. 3 shows a summary of the fit results to $Z \rightarrow b\bar{b}$ (left) in diboson production and to $H \rightarrow b\bar{b}$ in VH production (right). Results are shown separately for each year and each channel, as well as after the combination of both years. The $Z \rightarrow b\bar{b}$ decay is observed with a 4.8σ significance, and the ratio of its cross section to the expectation from the Standard Model is measured to be $\mu_{VZ} = 0.9 \pm 0.2$. The measured μ value for the Higgs boson decay is $0.2^{+0.7}_{-0.6}$. The measured μ is close to 1σ above $\mu = 0$ in 2012 data but a deficit in 2011 data that makes the combined measurement inconclusive.

Fig. 4 shows the exclusion limits at 95% confidence level (CL) as a function of the mass of the Higgs boson. The analysis is expected to be able to exclude $m_H < 117$ GeV. However, a slight

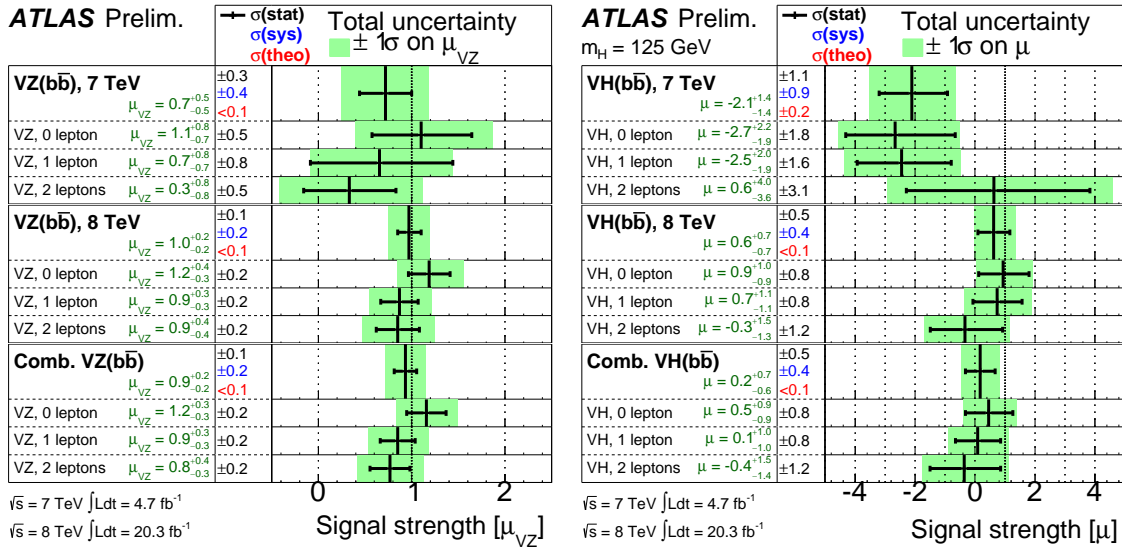


Figure 3: Fitted diboson signal strength μ_{VZ} (left) and Higgs boson signal strength μ (right) for the 7 TeV, 8 TeV, and combined datasets, and for the three channels separately and combined [10]. The individual values for the lepton channels are obtained from a simultaneous fit with the signal strength for each floating independently.

excess with respect to the background prediction in data does not allow for any observed exclusion in the mass range studied.

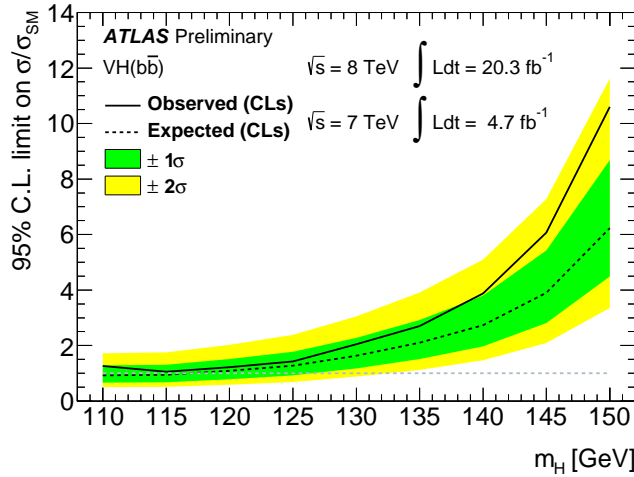


Figure 4: Expected (dashed) and observed (solid) 95% CL upper limits in the cross section, normalized to the SM Higgs boson production cross section, as a function of m_H for all channels and data taking periods combined [10]. The expected upper limit is given for the background-only hypothesis. The green and yellow bands represent the 1σ and 2σ ranges of the expectation in the absence of a signal.

6. Conclusions

This note has presented the search for associated production of a Higgs boson with a vector boson with the Higgs boson decaying to $b\bar{b}$ using the full Run 1 dataset collected by the ATLAS detector. The search is complemented by a measurement of the $VZ(Z \rightarrow b\bar{b})$ cross section, where $V = W, Z$. This decay is observed at the 4.8σ level, and its cross section is found to be consistent with that predicted by the SM. A small excess is observed in the search, which does not allow to exclude any Higgs boson mass in the range 110-150 GeV at the 95% confidence level. The ratio of the measured cross section to the expectation of the SM at $m_H = 125$ GeV is $\mu = 0.2^{+0.7}_{-0.6}$ consistent with both background-only and signal hypotheses. More data is needed to be conclusive in this channel.

References

- [1] ATLAS Collaboration, JINST 3 (2008) S08003
- [2] CMS Collaboration, JINST 3 (2008) S08004
- [3] ATLAS Collaboration, Phys.Lett. B716 (2012) 1-29, arXiv:1207.7214
- [4] CMS Collaboration, Phys.Lett. B716 (2012) 30-61, arXiv:1207.7235
- [5] ATLAS Collaboration, Phys. Lett. B726 (2013) 88-119, arXiv:1307.1427
- [6] ATLAS Collaboration, Phys. Lett. B726 (2013) 120-144, arXiv:1307.1432
- [7] CMS Collaboration, CMS-PAS-HIG-13-005, <https://cds.cern.ch/record/1542387>
- [8] A. Djouadi, J. Kalinowski and M. Spira, Comput. Phys. Commun. 108 (1998) 56-74, hep-ph/9704448
- [9] ATLAS Collaboration, ATLAS-CONF-2011-102, <https://cds.cern.ch/record/1369219>
- [10] ATLAS Collaboration, ATLAS-CONF-2013-079, <https://cds.cern.ch/record/1563235>
- [11] R. Barlow, Nucl. Inst. and Meth. A297 (1990) 496-506